

UNIVERSITY OF MARYLAND

UNDERGRADUATE THESIS

---

Ghostly Stellar Halos in Dwarf Galaxies

---

*Author:*

Hoyoung Kang

*Advisor:*

Dr. Massimo Ricotti

COMMITTEE MEMBERS:

Dr. Thomas Cohen

Dr. James Drake

February 2016

# *Abstract*

## **Ghostly Stellar Halos in Dwarf Galaxies**

Hoyoung Kang

*Department of Physics, University of Maryland*

Our study aims at probing the typical masses of the smallest and faintest galaxies that have ever formed in the universe. We carry out numerical simulations to characterize the size, stellar mass, and stellar mass surface density of stellar halos as a function of dark matter halo mass and a parameter that dictates the amount of stellar mass. We expect that for galaxies smaller than a critical value, these ghostly halos will not exist because the smaller galactic subunits that build it up, do not form any stars. Our results indicate the introduced parameter dominates the behaviors of stellar halos over dark matter mass. This indicates finding the appropriate parameter value is crucial to characterize these halos. We also find redshift contributes to the behavior of stellar mass but has no significant impact on the size of stellar halos.

# *Acknowledgements*

Throughout my undergraduate career, I have faced innumerable hardships and obstacles. Fortunately, I was able to overcome them with tremendous support from amazing people.

First and foremost I wish to express my sincerest appreciation and gratitude to my research mentor, Dr. Ricotti. When I expressed my immense interest in cosmology, he readily gave me this incredible project to work on. He patiently guided me through the project, always making sure I understood every step of the way. I truly thank him for all the hours he invested in me. I would like to thank my thesis committee, Drs. Cohen and Drake, for their encouragement, constructive comments, and thought provoking questions. I would also like to thank Dr. Wolfire for allowing me to access astronomy servers.

I could not have completed this thesis without the aid of my advisors and professors. My sincere thanks go to Drs. Dorland and Gates. They always treated my personal matters as their own and gave me valuable advice. I thank my academic advisor, Tom Gleason. He has facilitated my physics education academically, financially, and mentally. I also thank Drs. Orozco, Sau, Shawhan, and Yakovenko. They were excellent teachers who went above and beyond to help me succeed in their classes.

My final and deepest thanks go to my friends and family, especially Michaela, Sylvia, Mom, and Dad. Their unconditional love and support have motivated me to keep pushing through difficult times. Without them, I could not be where I am now.

Thank you all for believing in me. Your positive impacts have enabled me to complete this thesis.

# Contents

|          |  |           |
|----------|--|-----------|
| <b>1</b> | <b>Introduction</b>                            | <b>1</b>  |
| <b>2</b> | <b>Simulations</b>                             | <b>2</b>  |
| 2.1      | Stellar Halo Models . . . . .                  | 2         |
| 2.2      | Simulation Code and Model Parameters . . . . . | 4         |
| <b>3</b> | <b>Results and Discussion</b>                  | <b>5</b>  |
| 3.1      | Final Effective Radius . . . . .               | 5         |
| 3.2      | Stellar Mass . . . . .                         | 7         |
| 3.3      | Stellar Mass Surface Density . . . . .         | 9         |
| <b>4</b> | <b>Conclusion</b>                              | <b>11</b> |
| <b>A</b> | <b>Parameter Values</b>                        | <b>12</b> |
|          | <b>References</b>                              | <b>13</b> |

# 1 Introduction

Experiments and observations suggest dark matter exists. For example, the dynamics of galaxies indicates there should be more matter than what we see. Dark matter has zero luminosity and only interacts gravitationally [1]. In cold dark matter (CDM) cosmology, where the term "cold" refers to non-relativistic dark matter, galaxy formation is hierarchical: galaxies grow by accreting smaller mass galaxies. The accretion of these galaxies produce an extended stellar halo, with a luminosity that depends on how luminous the accreting galaxies are and a size that depends on the number of mergers. An extended stellar halo, which consists of stars and surrounds the galaxy, is followed by an even larger halo of dark matter. A stellar halo is observed around the Milky Way, but not much is known about stellar halos around dwarf galaxies. We define dwarf galaxies to have dark matter halo mass,  $M_{dm} < 10^{10} M_{\odot}$ . In a dwarf galaxy, most of stars in the stellar halo have formed in pre-reionization era and had little star formation since then. Such a dwarf galaxy is categorized as a "true fossil" [2]. Before reionization, the universe was said to be in "dark ages." Most of the matter in this era was dark matter and the universe was neutral i.e. no luminous objects had formed. Slowly, gravitational collapse of overdense regions of dark matter led to halo-like structure formations. As structure formation proceeded, temperature variations developed. This started the reionization era and first stars began to form. After reionization, redshift  $z \sim 6$ , gas in the universe became hot and the force from thermal pressure overcame gravitational pull for galaxies with dark matter halo mass,  $M_{dm} < 10^{10} M_{\odot}$ . Thus stellar halos around true fossils have an extremely low surface brightness and it is hard to observe them. Consequently, we call these dim halos, "ghostly halos" [3]. By studying its properties such as radius, stellar mass, stellar mass surface density, we may be able to answer the question of what the typical masses of the smallest and faintest galaxies are. Furthermore, we may be able to shed some light on puzzling questions of the origin of stars and how galaxies actually form.

## 2 Simulations

### 2.1 Stellar Halo Models

In order to estimate the increase of the stellar radius as a result of mergers, we adopt the formalism in [4, 5] used to describe the build up of bulges as a result of minor and major merger events. The final effective radius, radius at half of the total luminosity is emitted, of the stellar component in a binary merger of two galaxies,  $R_f$ , can be related to their initial radii  $R_1, R_2$  by the energy conservation:

$$f_f \frac{M_f^2}{R_f} = f_1 \frac{M_1^2}{R_1} + f_2 \frac{M_2^2}{R_2} + (f_{orb} + f_t) \frac{M_1 M_2}{R_1 + R_2}, \quad (2.1)$$

where  $M_1$  and  $M_2$  are initial masses of the stellar spheroids,  $M_f = M_1 + M_2$  is the final stellar halo mass,  $f_{orb}$  contains information about the orbital energy of the merger event, and  $f_t$  describes the energy transfer between the stellar and the dark matter components. The parameters of order of unity  $f_1, f_2$  and  $f_f$ , depend on the detail of the dark matter and stellar structure of the initial galaxies and the final galaxy, respectively. These parameters can only be obtained using numerical simulations as they encode both the gravitational potential energy and the internal kinetic energy of the galaxy.

However, if we assume perfect homology (i.e. the profiles of galaxies are the same up to scaling constants) and a parabolic orbit with no energy transfer between the dark matter and the stellar component, then  $f_f = f_1 = f_2$  and  $f_{orb} = f_t = 0$ , respectively [4, 6]. Then we get the following simplified equation:

$$\frac{M_f^2}{R_f} = \frac{M_1^2}{R_1} + \frac{M_2^2}{R_2}. \quad (2.2)$$

If we further assume constant radius for each initial halo mass and we consider merger of  $N$  galaxies,  $M_i$  for  $1 \leq i \leq N$ , then we can solve for  $R_f$ :

$$R_f = R_0 \frac{\left( \sum_{i=1}^N M_{*,i} \right)^2}{\sum_{i=1}^N M_{*,i}^2}. \quad (2.3)$$

Here  $R_0$  is the effective radius of the merging galaxies and  $M_{*,i}$  is their stellar mass. The stellar mass can be related to the total dark matter halo mass:

$$M_* = f_* M_{dm}, \quad (2.4)$$

where

$$f_* = \epsilon \left( \frac{M_{dm}}{M_0} \right)^\beta. \quad (2.5)$$

Parameter  $\beta$  is introduced to account for various possible stellar masses for a given dark matter mass. Parameters  $\epsilon$  and  $M_0$  correspond to the Milky Way galaxy and act as normalization factors in our models.

We now assume radius for each initial halo mass depends on dark matter halo mass. Thus, we assume  $R_i = R_0 \left( \frac{M_{dm,i}}{M_0} \right)^\alpha$  where  $\alpha = 1/3$ , which comes from the virial theorem that the radius of the stellar component is a constant fraction of the virial radius. Therefore, we obtain

$$R_f = R_0 \frac{\left( \sum_{i=1}^N \mu_i \right)^2}{\sum_{i=1}^N \mu_i^{2 - \frac{\alpha}{\beta+1}}}, \quad (2.6)$$

where

$$\mu \equiv M_*/\epsilon M_0. \quad (2.7)$$

Surface brightness of the stellar halo is related to luminosity and radius. Since our simulation contains no star formation, we assume  $M_* \propto L$  where  $L$  is luminosity. Then we can express surface brightness as stellar mass surface density:

$$\Sigma = \frac{L}{\pi R_f^2}, \quad (2.8)$$

$$\Sigma_{M_*} = \frac{M_*}{\pi R_f^2}. \quad (2.9)$$

## 2.2 Simulation Code and Model Parameters

In order to estimate  $R_f$  in equation (2.6) we need to know the merger history of a galaxy. We express today's mass of a galaxy in dark matter mass  $M_{dm}$ . We use a Monte-Carlo merger tree code [7] based on the extended Press-Schechter formalism to produce several realizations of the merger history of galaxies in halos of mass  $M_{dm}$ .

The merger tree code starts at some redshift  $z > 0$ . It creates  $n$  number of trees and merges smaller galaxies differently for each tree. Because there is no star formation, the total stellar mass is the sum of stellar components in the starting galaxies. At the end of the simulation, stellar mass is conserved and we expect a decrease in surface brightness.

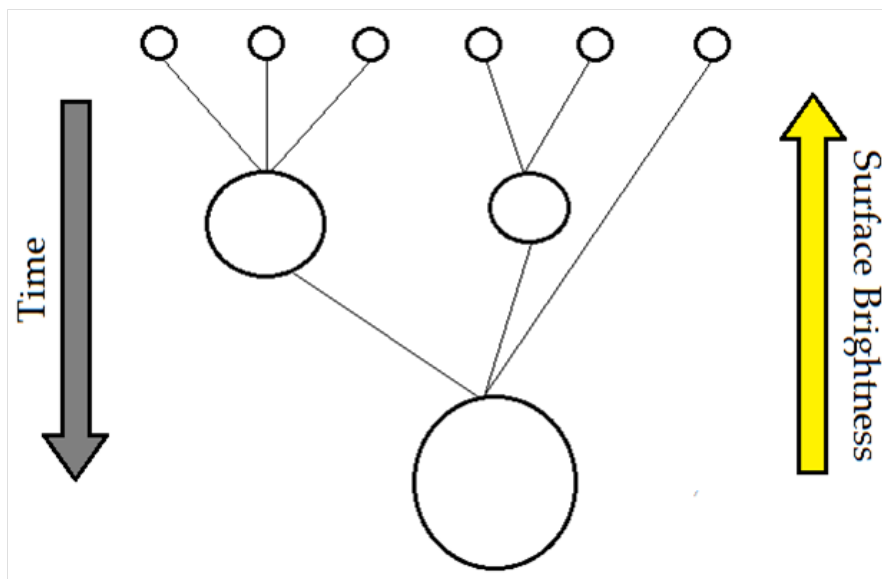


FIGURE 2.1: A schematic of a merger tree. Size of the nodes represent the size of the galaxies.

In our simulations, redshift values are chosen at  $z \sim 10$  and  $z \sim 6$  because reionization of the universe began around  $z \sim 10$  and ended around  $z \sim 6$ . Present day dark matter halo masses range from  $5 \times 10^9 M_\odot$  to  $10^{12} M_\odot$  to cover a wide range of dwarf galaxies up to the Milky Way ( $10^{12} M_\odot$ ). Parameter  $\beta$  broadly ranges from 0 to 2 based on current observational data which shows brightest galaxies have  $\beta = 0$  and faintest galaxies, that cannot be detected, have  $\beta = 2$ . We expect brightness of ghostly halos to fall within this range. Our simulation is further constricted by the mass resolution, which sets a limit to the smallest galaxy possible that can merge. Mass resolution,  $M_{res}$  is set at  $5 \times 10^6 M_\odot$ . Each simulation



run at each fixed parameter, mentioned above, creates 30 trees to account for different ways the final galaxy is formed and outputs the final effective radius and stellar mass surface density for each tree.

### 3 Results and Discussion

We carry out simulations to investigate how our parameters impact final effective radii of stellar halos, stellar masses, and stellar mass surface densities of merged galaxies. Each simulation data point is the average of 30 points (we have assumed Gaussian distribution among scatter points for the purpose of this study).

#### 3.1 Final Effective Radius

Fig. 3.1 and Fig. 3.2 represent final effective radii for different parameter values.

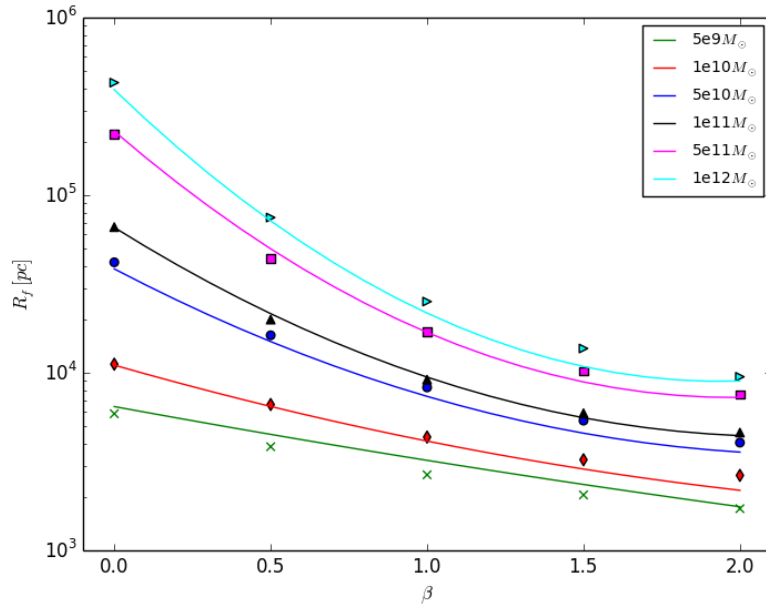


FIGURE 3.1: Average final effective radii profiles for redshift  $z \sim 10$ . Legends represent dark matter halo masses of the present day. Simulation data points are fit as a function of dark matter halo mass and  $\beta$ .

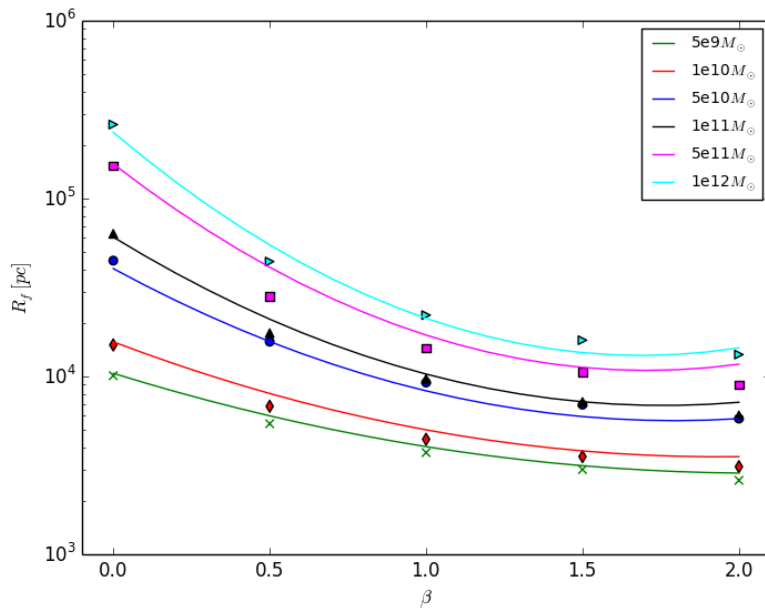


FIGURE 3.2: Same profiles as Fig 3.1 but for redshift  $z \sim 6$  instead.

We fit the data points as a function of dark matter halo mass normalized to the Milky Way mass and  $\beta$ :

$$R_f = R_{f,0} \left( \frac{M_{dm}}{M_0} \right)^{\gamma(\beta)}. \quad (3.1)$$

Our goal is to find  $R_{f,0}$  and  $\gamma$ . If we set  $M_{dm} = M_0$ , then  $R_f = R_{f,0}$ . However,  $M_0 = 10^{12} M_\odot$ . This allows us to use  $M_{dm} = 10^{12} M_\odot$  data points to find  $R_{f,0}$ :

$$R_{f,0} = 10^{a'\beta^2 + b'\beta + c'}. \quad (3.2)$$

We find  $\gamma$  in the following ways. We first fix  $\beta$  and fit as a function of  $M_{dm}$ . It turns out  $R_f \propto M_{dm}^\kappa$  where  $\kappa$  depends on  $\beta$ . We then take different values of  $\kappa$  and fit as a function of  $\beta$  using quadratic regression, which gives us  $\gamma(\beta)$ . Thus, we obtain the final form of (3.1), normalized to  $M_0$ :

$$R_f = R_{f,0} \left( \frac{M_{dm}}{M_0} \right)^{a\beta^2 + b\beta + c}. \quad (3.3)$$

We said the size of stellar halos depends on the number of mergers. By having a higher present day dark matter halo mass, it allows the simulation to have more mergers. Indeed, this is evident in the plots; we see larger halos for larger masses. It is interesting to note with no  $\beta$  dependence i.e.  $\beta = 0$ , effective radii of stellar halos vary significantly by dark matter halo mass. Once  $\beta$  is taken into an account, it dominates over the mass and final radii converge as  $\beta$  increases. This can be explained by examining (2.4) and (2.5), we see stellar mass depends exponentially on  $\beta$ . We get the largest stellar mass possible for  $\beta = 0$  and the smallest for  $\beta = 2$ .

## 3.2 Stellar Mass

We have assumed  $M_* \propto L$ . This corresponds to our code where no star formation occurs. Our simulations output final effective radii of stellar halos and stellar mass surface densities. Using (2.9), we find  $M_*$  and plot its dependence on  $\beta$  and  $M_{dm}$  as shown in Fig. 3.3 and Fig. 3.4.

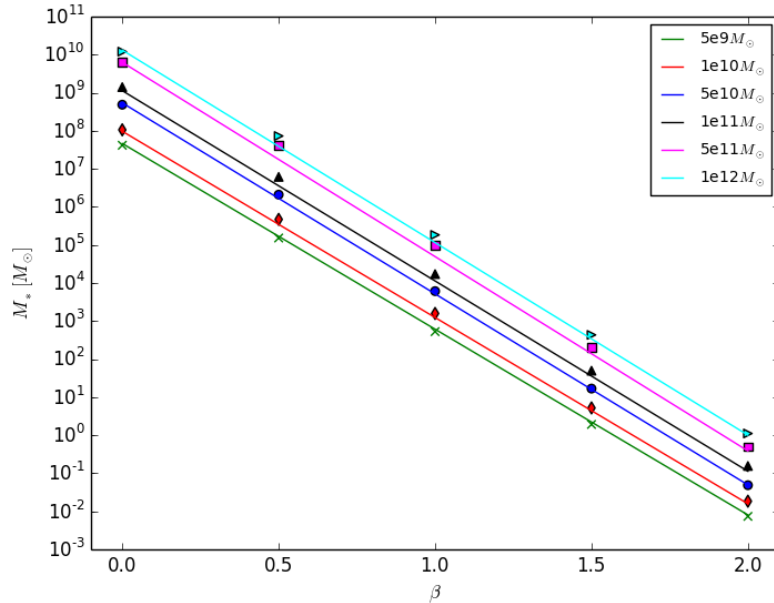


FIGURE 3.3: Average stellar mass profiles for redshift  $z \sim 10$ . Legends represent dark matter halo masses of the present day. Simulation data points are fit as a function of dark matter halo mass and  $\beta$ .

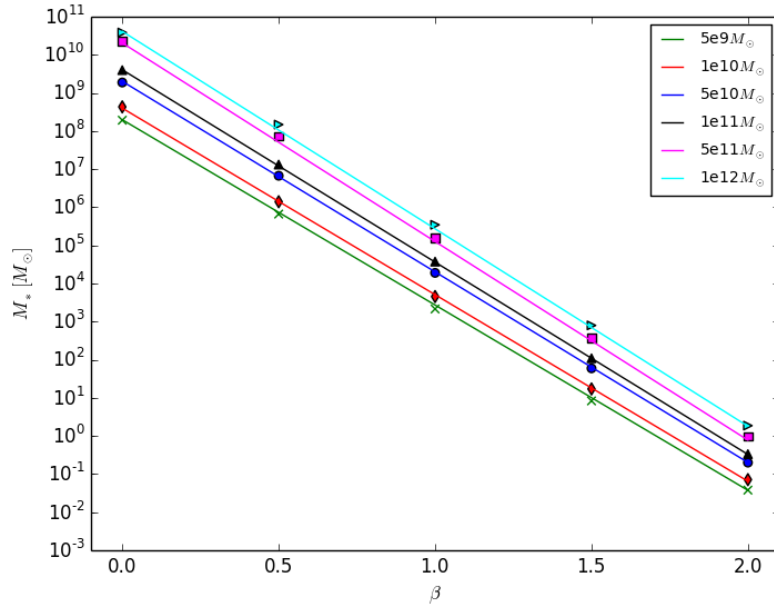


FIGURE 3.4: Same profiles as Fig 3.3 but for redshift  $z \sim 6$  instead.

We fit the data points as a function of dark matter halo mass normalized to the Milky Way mass and  $\beta$ :

$$M_* = M_{*,0} \left( \frac{M_{dm}}{M_0} \right)^{\kappa(\beta)}. \quad (3.4)$$

Our goal is to find  $M_{*,0}$  and  $\kappa$ . Here, we set  $\beta = 0$  to give us  $M_{*,0}$  that only depends on dark matter halo mass normalized to  $M_0$ :

$$M_{*,0} = 10^{12+c'''} \left( \frac{M_{dm}}{M_0} \right). \quad (3.5)$$

Now we fix dark matter halo mass and vary  $\beta$ . This gives us  $M_* \propto 10^{b'''\beta}$  where  $b'''$  varies with mass. Thus, we look at how  $b'''$  depends on mass to find  $\kappa(\beta)$  to find the final stellar mass model:

$$M_* = M_{*,0} 10^{c''\beta} \left( \frac{M_{dm}}{M_0} \right)^{b''\beta}. \quad (3.6)$$

At  $\beta = 0$ , we see stellar mass is directly proportional to dark matter mass. As  $\beta$  increases, we see slight convergence of  $M_*$ . This is more evident for  $z \sim 6$  than

for  $z \sim 10$ . However, this effect is not as crucial as the effect for final effective radii.

### 3.3 Stellar Mass Surface Density

We have fit data to effective radius and stellar mass models. Therefore, we use these models to derive the stellar mass surface density model using (2.9). This is a natural step to ensure each model can be derived from the other two. We find a stellar mass surface density model to fit its data points as shown in Fig. 3.5 and Fig. 3.6.

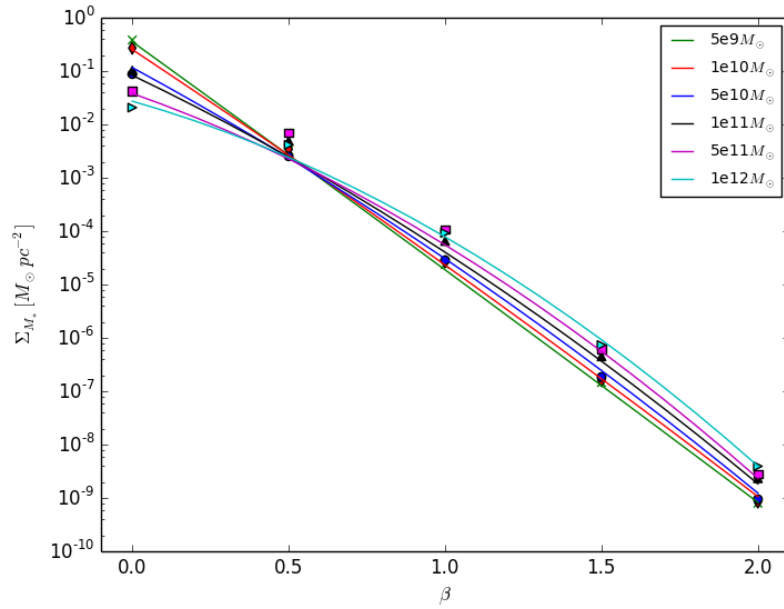


FIGURE 3.5: Average stellar mass surface density profiles for redshift  $z \sim 10$ . Legends represent dark matter halo masses of the present day. Simulation data points are fit as a function of dark matter halo mass and  $\beta$ .

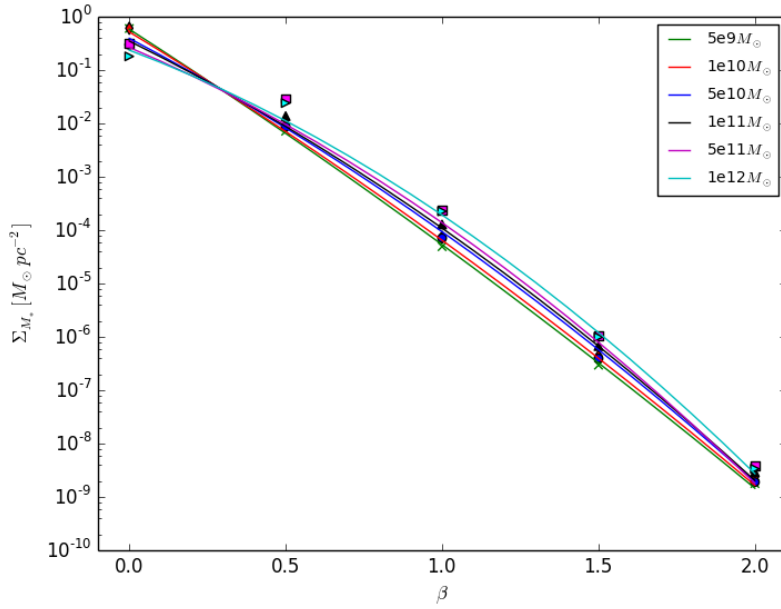


FIGURE 3.6: Same profiles as Fig 3.5 but for redshift  $z \sim 6$  instead.

$$\Sigma_{M_*} = M_{*,0} 10^{c''\beta} \left( \frac{M_{dm}}{M_0} \right)^{b''\beta} \frac{1}{\pi} \left[ \frac{1}{R_{f,0} \left( \frac{M_{dm}}{M_0} \right)^{a\beta^2 + b\beta + c}} \right]^2, \quad (3.7)$$

$$= \frac{1}{\pi} 10^{12 + c''' + c''\beta - 2(a'\beta^2 + b'\beta + c')} \left( \frac{M_{dm}}{M_0} \right)^{1 + b''\beta - 2(a\beta^2 + b\beta + c)}. \quad (3.8)$$

The overall scatter in stellar mass surface density is small compared to final effective radius and stellar mass. Some simulation points overlap the others which indicate stellar mass surface density may be independent of mass. For redshift  $z \sim 6$ , in particular, it seems mass dependence is minimal. We find our stellar mass surface density model fits worse than the previous models especially at  $\beta \sim 0.5$ . However, it is important to note we have assumed Gaussian distribution of simulation data; the model's validity cannot be concluded without taking the distribution of the scatter into an account. Also, we fit stellar mass surface density using two previous models where they too had some discrepancies. In addition, it is interesting the fitted lines all intersect at one point. This may be a consequence from combining our radius and stellar mass models.

## 4 Conclusion

In this thesis, we have characterized stellar halos in dwarf galaxies. We fitted simulation data to our models as a function of dark matter halo mass and a parameter  $\beta$  which determines how much stellar mass we expect for a given dark matter halo mass. As we have expected, with no star formation, all three characterizations of stellar halos decrease as  $\beta$  increases. Additionally, as  $\beta$  increases, it dominates the behavior of these characterizations over dark matter halo mass.

From our simulations, we have found the size of stellar halos is independent of redshift. Redshift's significance becomes more evident in stellar mass with stellar mass accumulated from  $z \sim 6$  being greater than that from  $z \sim 10$  by a factor of  $\sim 3$ . Since we know the relationship between the size of stellar halos and the stellar mass, we then expect the ratio of stellar mass surface density for  $z \sim 6$  and  $z \sim 10$  to be  $\sim 3$ . Indeed, this is evident in our graphs. Redshift also has an impact on the dark matter halo mass dependence of the three characterizations we have explored. At each  $\beta$ , simulation data points are less scattered for  $z \sim 6$  than for  $z \sim 10$ . This is most likely due to the fact that we can expect more possible ways galaxies can merge for higher redshift. This tells us as we get to lower redshift, mass dependence becomes more trivial.

In the future, these models could be tested by comparing with observational data. This could potentially direct us towards finding  $\beta$  value that corresponds with the behavior of ghostly halos. Then, dark matter mass would be varied at the fixed  $\beta$  which could be used to determine the typical masses of the smallest and faintest galaxies that have ever formed. Another area to examine is distribution of simulation data points. Distribution will indicate the accuracy of simulation data points since, in this study, we have assumed a Gaussian shape. Also, significance of redshift will be further examined by looking at other redshifts. Finally, the intersection point of stellar mass surface density lines will be investigated to provide a physical meaning to it.

## A Parameter Values

| Parameters | Values  | Errors       |
|------------|---------|--------------|
| $c'''$     | -2.6780 | $\pm 0.3432$ |
| $b''$      | -0.0925 | $\pm 0.0171$ |
| $c''$      | -5.0993 | $\pm 0.0243$ |
| $a'$       | 0.4377  | $\pm 0.0437$ |
| $b'$       | -1.6954 | $\pm 0.0912$ |
| $c'$       | 5.5936  | $\pm 0.0385$ |
| $a$        | 0.1812  | $\pm 0.0343$ |
| $b$        | -0.5962 | $\pm 0.0716$ |
| $c$        | 0.7752  | $\pm 0.0302$ |

TABLE A.1: Listed are the parameter values for final effective radius, stellar mass, and stellar mass surface density for redshift  $z \sim 10$

| Parameters | Values  | Errors       |
|------------|---------|--------------|
| $c'''$     | -1.4683 | $\pm 0.2032$ |
| $b''$      | -0.1550 | $\pm 0.0143$ |
| $c''$      | -5.2105 | $\pm 0.0203$ |
| $a'$       | 0.4398  | $\pm 0.0996$ |
| $b'$       | -1.4854 | $\pm 0.2077$ |
| $c'$       | 5.3723  | $\pm 0.0877$ |
| $a$        | 0.1339  | $\pm 0.0366$ |
| $b$        | -0.4092 | $\pm 0.0764$ |
| $c$        | 0.5888  | $\pm 0.0323$ |

TABLE A.2: Same parameters as Table A.1, but for redshift  $z \sim 6$  instead



# References

- [1] J. Einasto. Dark Matter: Early Considerations. In A. Blanchard and M. Signore, editors, *Frontiers of Cosmology*, page 241, January 2005.
- [2] M. Ricotti and N. Y. Gnedin. Formation Histories of Dwarf Galaxies in the Local Group. *ApJ*, 629:259–267, August 2005.
- [3] M. S. Bovill and M. Ricotti. Where are the Fossils of the First Galaxies? II. True Fossils, Ghost Halos, and the Missing Bright Satellites. *ApJ*, 741:18, November 2011.
- [4] M. Boylan-Kolchin, C.-P. Ma, and E. Quataert. Dissipationless mergers of elliptical galaxies and the evolution of the fundamental plane. *MNRAS*, 362:184–196, September 2005.
- [5] M. Boylan-Kolchin, C.-P. Ma, and E. Quataert. Red mergers and the assembly of massive elliptical galaxies: the fundamental plane and its projections. *MNRAS*, 369:1081–1089, July 2006.
- [6] G. S. Novak, P. Jonsson, J. R. Primack, T. J. Cox, and A. Dekel. On galaxies and homology. *MNRAS*, 424:635–648, July 2012.
- [7] H. Parkinson, S. Cole, and J. Helly. Generating dark matter halo merger trees. *MNRAS*, 383:557–564, January 2008.